MATHEMATICAL BIOSCIENCES
AND ENGINEERING
Volume **12**, Number **3**, June **2015**

doi:10.3934/mbe.2015.12.537

pp. **537–554**

CELL SCALE MODELING OF ELECTROPERMEABILIZATION BY PERIODIC PULSES

Michael Leguèbe

Inria Bordeaux Sud-Ouest
200, Rue de la Veille Tour
33405 Talence, France
Current address : Max Planck Institute for Solar System Research
Justus-von-Liebig-Weg 6
37077 Göttigen, Germany

(Communicated by Sharon Crook)

Abstract. In this paper, we focus on the behaviour of periodic solutions to a cell-scale electropermeabilization model previously proposed by Kavian *et al.* [6]. Since clinical permeabilization protocols mostly submit cancer cells to trains of periodic pulses, we investigate on parameters that modify significantly the resulting permeabilization. Theoretical results of existence and uniqueness of periodic solutions are presented, for two different models of membrane electric conductivity. Numerical simulations were performed to corroborate these results and illustrate the asymptotic convergence to periodic solutions, as well as the dependency on biological parameters such as the cell size and the extracellular conductivity.

1. **Introduction.** *Electropermeabilization* or *electroporation* is a phenomenon that occurs when a biological cell or a lipid vesicle is submitted to a high electric field. If a sufficiently large potential difference is applied to the membrane, its structure is altered and molecules that are usually not able to enter the cytoplasm can diffuse inside the cell. Reversible electropermeabilization is already used to improve delivery of drugs such as bleomycin in oncology [1, 4], and also to make the cell permeable to very large molecules for gene transfer [11].

This paper is an extension of a previous modeling work [6] in which we proposed a phenomenological approach to electropermeabilization, in comparison with the previous most achieved models of Neu, Debruin and Krassowska [13, 3].

Experiments show that a single electric impulsion is often not sufficient to achieve cell electropermeabilization, with a wide variety of pulses, from nanopulses to millipulses [12, 20, 19]. The electric field is therefore usually applied by trains of several pulses, which can be considered as a periodic source. Here we focus theoretically and numerically on the behaviour of solutions to our equations in this particular case of sources. The objective of this paper is to show that the membrane conductivity reaches a stable periodic state when submitted to a periodic voltage.

Generally, electroporation models at cell scale mainly focus on the evolution of the transmembrane potential [3, 5, 10]. The relationship between the conductivity

2010 *Mathematics Subject Classification.* Primary: 35Q92, 35Q60; Secondary: 92B05, 92C05.
Key words and phrases. Cell modeling, electropermeabilization, non-linear partial differential equations.

of the membrane and its actual degree of permeability may however be non-trivial. We proposed a model [9] in which membrane permeabilization is triggered when a porosity threshold is exceeded (see equations 4,8 and 9), corresponding to an activation conductivity. As the underlying mechanisms of lipids permeabilization are not clearly determined at the biophysical level yet, we used the same phenomenological modeling approach as for the membrane poration. It is also possible to link directly the permeability to the electric potential as proposed in [7] (page 97, equation 4.7), in particular for pulses of several milliseconds. Both permeability models give qualitative results that are in agreement with experiments, and calibration of these will be forthcoming work. However, in both cases, studying the electric potential evolution and the resulting conductivity is necessary to determine the resulting degree of permeability of the whole cell.

When very intense electric pulses are clinically applied, healthy tissues in the vicinity of the electrodes are completely damaged due to the high electric field. Moreover, thermal effects induce cell destruction if pulses last for too long. It is therefore important to determine pulse characteristics (voltage, duration) that are sufficient to permeabilize the targeted tissue, minimizing at the same time the caused damage. Considering that, we will focus on the amount of time needed for the cell to reach a periodic conductive state, depending on which model is chosen to describe the membrane conductivity.

We will show, in particular, that using a static model of conductivity results in a high convergence speed of the solution to a periodic state. A first conclusion should be that a few pulses are needed to reach it. However, results given by a fully dynamical model infer that more pulses are required to actually achieve electropermeabilization.

After recalling in the first section the model of the electric potential in a biological cell, and especially across its membrane, we will justify the existence and uniqueness of periodic solutions in the second section. In the final section, we will illustrate how a cell at rest submitted to a periodic source reaches a periodic state. We will validate these results with numerical simulations.

2. Statement of the model.

2.1. The electric potential in a biological cell.

A biological cell is considered as an homogeneous medium $\mathcal{O}_{\mathrm{c}}$, which is separated from an exterior bath $\mathcal{O}_{\mathrm{e}}$ by a phospholipidic membrane Γ (see fig. 1). Due to the high resistivity and the thickness of the membrane, it is considered as a single surface interface between the two domains.

Notation.

- We denote by $\boldsymbol{n}$ the unit vector normal to the surface Γ (or curve in $\mathbb{R}^2$), outwardly directed from $\mathcal{O}_{\mathrm{c}}$ to $\mathcal{O}_{\mathrm{e}}$.
- Let f be a smooth function defined in a neighborhood of Γ. The values of f on each side of Γ are defined by:

$$\forall x \in \Gamma,\ f_{|\Gamma^{\pm}}(x) := \lim_{\tau \to 0^{\pm}} u(x \pm \tau \boldsymbol{n}(x)).$$

Then we denote the jump of f across the interface by:

$$[f(x)]_{\Gamma} := f_{|\Gamma^{+}}(x) - f_{|\Gamma^{-}}.$$

The flux of f across the interface is defined by:

$$\forall x \in \Gamma,\ \partial_{\boldsymbol{n}} f_{|\Gamma^{\pm}}(x) = \lim_{\tau \to 0^{\pm}} \nabla f(x \pm \tau \boldsymbol{n}(x)) \cdot \boldsymbol{n}(x).$$

- We note $PH^1(\Omega)$ the space of functions whose restrictions on each subdomain belong to H^1:

$$PH^1(\Omega) := \left\{ f \in L^2(\Omega),\ f_{|\mathcal{O}_\mathrm{e}} \in H^1(\mathcal{O}_\mathrm{e}),\ f_{|\mathcal{O}_\mathrm{c}} \in H^1(\mathcal{O}_\mathrm{c}) \right\}.$$

The capacity of the membrane electric material is denoted by C_m, and its surface conductivity by S_m. Let σ be the conductivity of the medium, considered piecewise constant:

$$\sigma = \begin{cases} \sigma_\mathrm{e} & \text{in the bath } \mathcal{O}_\mathrm{e}, \\ \sigma_\mathrm{c} & \text{in the cytoplasm } \mathcal{O}_\mathrm{c}. \end{cases} \tag{1}$$

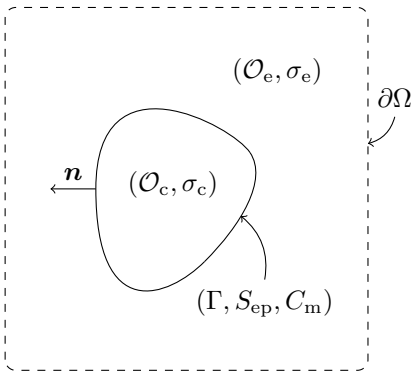

FIGURE 1. Geometry of the problem. The whole domain Ω is defined by $\Omega = \mathcal{O}_\mathrm{e} \cup \overline{\mathcal{O}_\mathrm{c}}$.

The electric potential U in both intra- and extracellular domains follows Poisson's law:

$$\Delta U = 0 \quad \text{in } \mathcal{O}_\mathrm{e} \cup \mathcal{O}_\mathrm{c}, \tag{2a}$$

$$U = g \quad \text{on } \partial\Omega,\ \forall t > 0, \tag{2b}$$

with the transmission conditions on the flux and the transmembrane potential across the interface Γ:

$$[\sigma \partial_{\boldsymbol{n}} U]_\Gamma = 0, \tag{2c}$$

$$C_\mathrm{m} \partial_t [U]_\Gamma + I_\mathrm{ep} = \sigma_\mathrm{c} \partial_{\boldsymbol{n}} U|_{\Gamma^-}, \tag{2d}$$

where g represents the potential that is applied by external electrodes, and I_ep is the total current due to electropermeabilization. Equation (2c) describes the continuity of the current across the membrane, whereas equation (2d) is a Kirchhoff's law describing the evolution of the local transmembrane potential difference. The discontinuity of the potential comes from the fact that we consider a membrane with no thickness. An asymptotic expansion of Poisson's law on a domain including the membrane leads to (2d), as performed in [14, 16].

In the most achieved models of electroporation proposed by Neu, Krassowska and De Bruin [13, 3], the current I_ep is defined as the product of a pore density N_ep by the current flowing through a single pore i_ep. The pore current is defined by a highly non-linear function of the transmembrane potential.

We proposed in our previous work [6] to define I_ep as the product of the surface conductivity of the membrane S_m by the transmembrane potential difference $[U]_\Gamma$,

which can be seen as a linearization of the current of the model of Neu *et al.* The transmission condition now holds :

$$C_{\mathrm{m}}\partial_t[U]_\Gamma + S_{\mathrm{m}}[U]_\Gamma = \sigma_{\mathrm{c}}\partial_{\boldsymbol{n}}U|_{\Gamma^-}. \tag{3}$$

In order to take into account electropermeabilization, we write S_{m} as the sum of the lipid conductivity at rest S_0 and a non-linear surface conductivity S_{ep} depending on $[U]_\Gamma$:

$$S_{\mathrm{m}}([U]_\Gamma) := S_0 + S_{\mathrm{ep}}([U]_\Gamma). \tag{4}$$

The next section introduces the different conductivity models we chose.

2.2. **Models of membrane conductivity.** Throughout this paper, we will focus on two models of membrane conductivity. We proposed these *ad hoc* models in [6], with the thought of reducing the number of parameters to facilitate the inverse problem resolution. As the rise of the electric membrane conductivity has not been clearly explained by experiments yet, we prefered to use a phenomenological approach, rather than performing an homogeneization of the description of a nanoscale mechanism. The voltage threshold is kept, as it is highlighted by all experiments and previous electroporation models.

- The first model is a static definition of conductivity, which has a sigmoid profile:

  $$\forall \lambda \in \mathbb{R},\ S_{\mathrm{ep}}(\lambda) = S_1\beta(\lambda), \quad \text{with } \beta(\lambda) = (1+\tanh(k_{\mathrm{ep}}(|\lambda| - V_{\mathrm{th}})))/2 \tag{5}$$

  where S_1 is another conductivity constant, much larger than S_0. k_{ep} defines the speed of the switch between the rest state ($S_{\mathrm{m}} = S_0$) and the fully permeabilized state ($S_{\mathrm{m}} = S_0 + S_1$). V_{th} designates the voltage threshold that needs to be crossed to permeabilize the membrane.

  We will refer to this model as the β-model.

Remark 1. The choice of the β function is not restricted to hyperbolic tangents. We showed that in a more general way, this function must satisfy the following conditions:

$$\begin{cases} \beta \in C(\mathbb{R}), \\ \lambda \mapsto \beta(\lambda) \text{ is even on } \mathbb{R}, \\ 0 < S_0 \leq \beta(\lambda) \leq 1, \\ \beta \text{ is non decreasing on } [0, +\infty), \\ \lim\limits_{\lambda \to +\infty} \beta(\lambda) = 1. \end{cases}$$

It is in particular possible to consider another threshold criterion, such as an electrostatic energy level, required to induce pore formation:

$$\beta(\lambda) = \exp\left(-\frac{E_{\mathrm{th}}}{\lambda^2}\right).$$

- The second conductivity definition is a dynamical model which will be called X-model: for $t \geqslant 0$,

  $$S_{\mathrm{ep}}(t,\lambda) = S_1 X(t,\lambda), \quad \text{with } \begin{cases} \partial_t X([U(t)]_\Gamma, t) = \dfrac{\beta([U(t)]_\Gamma) - X(t)}{\tau_{\mathrm{ep}}}, \\ X(t=0) = X_0 \in [0,1]. \end{cases} \tag{6}$$

  where β is the same function as the β-model and τ_{ep} is the characteristic time constant of formation and resealing of pores. The X variable follows an electrophysiology *sliding-door* model around the electropermeabilization

threshold V_{th}. When the transmembrane potential difference $[U]_\Gamma$ is high enough, then $\beta([U]_\Gamma) - X$ is positive and porosity rises with a dynamic τ_{ep}. On the contrary, when the pulse is cut or when the membrane conductivity is high, $\beta([U]_\Gamma) - X$ becomes negative, and the membrane tries to reseal with the same characteristic time. Using this model makes the dynamic of electropermeabilization intrisic to the cell and not dependent of the applied pulse.

We showed in [6] that X verifies:

$$\begin{cases} X \in C([0,+\infty)), \\ 0 \leqslant X(t,\lambda) \leqslant 1 \ \forall t \geqslant 0. \end{cases} \tag{7}$$

In addition, we showed that there exists $K > 0$ such that:

$$\forall t \geqslant 0, \ |\lambda_1 X(t,\lambda_1) - \lambda_2 X(t,\lambda_2)| \leqslant K|\lambda_1 - \lambda_2|. \tag{8}$$

As the functions β and X take values that are between 0 and 1, they can be considered as a description of the local degree of porosity of the membrane. $\beta = 0$ or $X = 0$ stands for a membrane at rest, whereas β or $X = 1$ corresponds to a membrane that would have been completely porated, at the limit between reversible and irreversible electroporation. Both these models fall in the hypothesis of theorem 10 in [6], so existence and uniqueness of solutions to problem (2) holds.

The main topic is now to know if given a periodic source term g, there exists a unique solution that is also periodic. Also, starting from any initial condition, does the solution converge to the periodic state, and at which speed ?

3. Existence and uniqueness of periodic solutions.

Notation. For any functionnal space H and $T > 0$, we will designate by $C_T(H)$ the subspace of functions of $C([0,+\infty), H)$ that are T-periodic :

$$C_T(H) = \{f \in C([0,+\infty), H), \forall t \geqslant 0, f(t+T,.) = f(t,.)\}.$$

This section will be dedicated to the proof of the following theorem :

Theorem 3.1. *Let $T > 0$ and g be a T-periodic function of $C_T(H^1(\partial\Omega)) \cap W^{1,1}((0,+\infty), L^2(\partial\Omega))$. There exists a unique T-periodic solution U to the following problem:*

$$\begin{cases} U \in C_T(PH^1(\Omega)), & \\ \Delta U = 0 & \text{in } \mathcal{O}_{\text{e}} \cup \mathcal{O}_{\text{c}}, \\ U = g & \text{in } \partial\Omega, \ \forall t \geqslant 0, \\ [\sigma \partial_{\boldsymbol{n}} U]_\Gamma = 0, & \\ C_{\text{m}} \partial_t [U]_\Gamma + S_0 [U]_\Gamma + S_{\text{ep}}(t, [U]_\Gamma)[U]_\Gamma & = \sigma_{\text{c}} \partial_{\boldsymbol{n}} U|_{\Gamma^-} \end{cases} \tag{9}$$

Also, let $V_0 \in PH^1(\Omega)$ and V be the solution to

$$\begin{cases} V \in C([0,+\infty), PH^1(\Omega)), & \\ \Delta V = 0 & \text{in } \mathcal{O}_{\text{e}} \cup \mathcal{O}_{\text{c}}, \\ V = g & \text{on } \partial\Omega, \ \forall t \geqslant 0, \\ V(t=0,.) = V_0(.) & \text{in } \Omega, \\ [\sigma \partial_{\boldsymbol{n}} V]_\Gamma = 0, & \\ C_{\text{m}} \partial_t [V]_\Gamma + S_0 [U]_\Gamma + S_{\text{ep}}(t, [V]_\Gamma)[V]_\Gamma & = \sigma_{\text{c}} \partial_{\boldsymbol{n}} V|_{\Gamma^-} \end{cases} \tag{10}$$

then, for all $t \geqslant 0$,

$$\|[U(t)]_\Gamma - [V(t)]_\Gamma\|^2_{L^2(\Gamma)} \leqslant e^{-\frac{C}{C_{\text{m}}} t} \|[U_0]_\Gamma - [V_0]_\Gamma\|^2_{L^2(\Gamma)}, \tag{11}$$

where C is a real constant.

C determines the convergence speed of a non-periodic solution towards the periodic solution to problem 9. It will be evaluated in the next section.

Proof. Existence and uniqueness of the solution V is given by [6]. In order to prove existence and uniqueness of periodic solutions to problem (9), we introduce the Dirichlet-to-Neumann (or Steklov-Poincaré) operators Λ_c and Λ_e on the interface for the Laplacian. Denote by $\boldsymbol{\nu_c}$ (resp. $\boldsymbol{\nu_e}$) the unitary normal to Γ directed from the inside to the outside of $\mathcal{O}_c$ (resp. $\mathcal{O}_e$). Λ_c and Λ_e are defined by:

$$\begin{array}{rccl} \Lambda_c & : & H^1(\Gamma) & \to & L^2(\Gamma) \\ & & f & \mapsto & \boldsymbol{\nu_c} \cdot \sigma_c \nabla U_c|_{\Gamma^-} \end{array} \quad \text{where} \quad \begin{cases} \nabla \cdot (\sigma_c \nabla U_c) = 0 \text{ in } \mathcal{O}_c, \\ U_c|_\Gamma = f. \end{cases} \tag{12a}$$

$$\begin{array}{rccl} \Lambda_e & : & H^1(\Gamma) & \to & L^2(\Gamma) \\ & & f & \mapsto & \boldsymbol{\nu_e} \cdot \sigma_e \nabla U_e|_{\Gamma^+} \end{array} \quad \text{where} \quad \begin{cases} \nabla \cdot (\sigma_e \nabla U_e) = 0 \text{ in } \mathcal{O}_e, \\ U_e|_{\partial\Omega} = 0, \\ U_e|_\Gamma = f. \end{cases} \tag{12b}$$

Using these operators, the transmission condition (2d) of the transmembrane potential can be rewritten on the manifold Γ. For the sake of readability, we now denote by u the transmembrane potential difference $[U]_\Gamma$ across the membrane. The condition now reads:

$$C_m \partial_t u + \Lambda_c (\mathrm{Id} + \Lambda_e^{-1}\Lambda_c)^{-1} u + S_0 u + S_{ep}(u)u = G, \tag{13}$$

where $G = \Lambda_c \left(\mathrm{Id} + \Lambda_e^{-1}\Lambda_c\right)^{-1} \Lambda_e^{-1}\Lambda_0 g$ is the external source term which has been brought to the interface *via* another Steklov-Poincaré operator:

$$\begin{array}{rccl} \Lambda_0 & : & H^1(\partial\Omega) & \to & L^2(\Gamma) \\ & & g & \mapsto & \boldsymbol{\nu_e} \cdot \sigma_e \nabla U_e|_{\Gamma^+} \end{array} \quad \text{where} \quad \begin{cases} \nabla \cdot (\sigma_e \nabla U_e) = 0 \text{ in } \mathcal{O}_e, \\ U_e|_{\partial\Omega} = g, \\ U_e|_\Gamma = 0. \end{cases} \tag{14}$$

Let $\mathcal{A} := \Lambda_c(\mathrm{Id} + \Lambda_e^{-1}\Lambda_c)^{-1}$, associating the current across Γ to a given transmembrane potential. In [6], we have already proven that the operator $(H^1(\Gamma), \mathcal{A})$ is m-accretive.

In order to prove the existence of periodic solutions, it is necessary to verify firstly the boundedness of the solution u to the following problem, equivalent of (2):

$$u \in C([0, +\infty), H^1(\Gamma)), \tag{15a}$$

$$C_m \partial_t u + \mathcal{A}u + S_0 u + S_{ep}(t, u)u = G, \text{ on } \Gamma, \forall t > 0 \tag{15b}$$

$$u(t = 0, .) = u_0(.) \text{ on } \Gamma. \tag{15c}$$

where $G \in C([0, +\infty), H^1(\Gamma))$ is not necessarily T-periodic, $u_0 \in H^1(\Gamma)$, $\mathcal{A}$ is a m-accretive operator and S_{ep} the conductivities previously defined in eqs. (5) and (6). We have, for all $t > 0$,

$$\langle C_m \partial_t u, u\rangle + \langle \mathcal{A}u, u\rangle + S_0\langle u, u\rangle + \langle S_{ep}(t, u)u, u\rangle = \langle G, u\rangle. \tag{16}$$

It is clear that for both conductivity models $\langle S_{ep}(t, u)u, u\rangle$ is positive. Hence thanks to Young's inequality:

$$\frac{1}{2} C_m \partial_t \|u\|^2_{L^2(\Gamma)} + \langle Au, u\rangle + S_0 \|u\|^2_{L^2(\Gamma)} \leqslant \frac{\|u\|^2_{L^2(\Gamma)}}{2\alpha} + \frac{\alpha G_\infty^2}{2}$$

for any $\alpha > 0$, with $G_\infty := \max_{t\in[0,T]} \|G(t)\|_{L^2(\Gamma)}$. Since $\mathcal{A}$ is m-accretive,

$$\frac{1}{2}C_{\mathrm{m}}\partial_t \|u\|^2_{L^2(\Gamma)} + S_0 \|u\|^2_{L^2(\Gamma)} \leqslant \frac{\|u\|^2_{L^2(\Gamma)}}{2\alpha} + \frac{\alpha G_\infty^2}{2}.$$

We can now invoque Gronwall's lemma to prove boundedness of solutions in finite times: $\forall t > 0$,

$$\begin{aligned}\|u(t)\|^2_{L^2(\Gamma)} &\leqslant \|u_0\|^2_{L^2(\Gamma)} \exp\left(-\frac{2\alpha S_0 - 1}{\alpha C_{\mathrm{m}}}t\right) + \frac{\alpha G_\infty^2}{C_{\mathrm{m}}}\int_0^t \exp\left(-\frac{2\alpha S_0 - 1}{\alpha C_{\mathrm{m}}}(t-s)\right) \mathrm{d}s,\\ &\leqslant \|u_0\|^2_{L^2(\Gamma)} \exp\left(-\frac{2\alpha S_0 - 1}{\alpha C_{\mathrm{m}}}t\right) + \frac{\alpha^2 G_\infty^2}{2\alpha S_0 - 1}\left(1 - \exp\left(-\frac{2\alpha S_0 - 1}{\alpha C_{\mathrm{m}}}t\right)\right).\end{aligned}$$

Setting $\alpha = \dfrac{1}{S_0}$ minimizes the coefficient $\dfrac{\alpha^2}{2\alpha S_0 - 1}$. Therefore,

$$\forall t > 0,\ \|u(t)\|^2_{L^2(\Gamma)} \leqslant \|u_0\|^2 \exp\left(-\frac{S_0}{C_{\mathrm{m}}}t\right) + \frac{G_\infty^2}{S_0^2}\left(1 - \exp\left(-\frac{S_0}{C_{\mathrm{m}}}t\right)\right). \tag{17}$$

Now that we have proven boundedness of solutions in finite times, we will focus on the existence and uniqueness of periodic solutions. Let G be a T-periodic source in $C_T(H^1(\Gamma))$, and $\mathcal{A}$ a m-accretive operator in $\mathcal{L}(H^1(\Gamma))$. We will show that there exists a unique periodic solution u satisfying :

$$\begin{cases} u \in C_T(H^1(\Gamma)), \\ C_{\mathrm{m}}\partial_t u + \mathcal{A}u + S_0 u + S_{\mathrm{ep}}(t,u)u = G. \end{cases} \tag{18}$$

Let u_0 and $v_0 \in H^1(\Gamma)$ be two initial states and u, v the associated solutions to problem (18). Let $w = u - v$. w satisfies the homogeneous problem:

$$\begin{cases} C_{\mathrm{m}}\partial_t w + \mathcal{A}w + S_0 w + S_{\mathrm{ep}}(t,u)u - S_{\mathrm{ep}}(t,v)v = 0, \\ w(t=0,.) = w(T,.) = u_0(.) - v_0(.). \end{cases} \tag{19}$$

We have, for $t \geqslant 0$,

$$C_{\mathrm{m}}\partial_t \|w\|^2_{L^2(\Gamma)} + \langle \mathcal{A}w, w\rangle + S_0 \|w\|^2_{L^2(\Gamma)} + \langle S_{\mathrm{ep}}(t,u)u - S_{\mathrm{ep}}(t,v)v, u - v\rangle = 0, \tag{20}$$

and since $\mathcal{A}$ is m-accretive,

$$C_{\mathrm{m}}\partial_t \|w\|^2_{L^2(\Gamma)} + S_0 \|w\|^2_{L^2(\Gamma)} + \langle S_{\mathrm{ep}}(t,u)u - S_{\mathrm{ep}}(t,v)v, u - v\rangle \leqslant 0. \tag{21}$$

In order to show that the difference $w(t)$ is decreasing in $\|.\|_{L^2(\Gamma)}$ norm, we will show that for each conductivity model, the term $\langle S_{\mathrm{ep}}(t,u)u - S_{\mathrm{ep}}(t,v)v, u - v\rangle$ is positive.

- In the case of the β-model, it is easy to verify that for any (λ_1, λ_2) with $\lambda_1 \neq 0$, the quantity

  $$(\beta(\lambda_1)\lambda_1 - \beta(\lambda_2)\lambda_2)(\lambda_1 - \lambda_2) = \beta(\lambda_1)\lambda_1^2\left(1 - \frac{\lambda_2}{\lambda_1}\right)\left(1 - \frac{\beta(\lambda_2)\lambda_2}{\beta(\lambda_1)\lambda_1}\right)$$

  is positive, since β is an increasing function on $[0, +\infty)$.
- For the X-model, the ODE

  $$\frac{\mathrm{d}}{\mathrm{d}s}X(s,\lambda(t)) = \frac{\beta(\lambda(t)) - X(s,\lambda(t))}{\tau_{\mathrm{ep}}},$$

  has the following solution

  $$X(s,\lambda(t)) = e^{-\frac{s}{\tau_{\mathrm{ep}}}}X(t,\lambda(t)) + \frac{\beta(\lambda(t))}{\tau_{\mathrm{ep}}}\int_0^s e^{-\frac{s-s'}{\tau_{\mathrm{ep}}}}\,\mathrm{d}s'.$$

Therefore the mapping $\lambda \mapsto \lambda X(t, \lambda(t))$ is monotone. Using the same argument as for the β-model, we infer that for all (λ_1, λ_2), $\lambda_1 \neq 0$

$$(X(\lambda_1)\lambda_1 - X(\lambda_2)\lambda_2)(\lambda_1 - \lambda_2) = X(\lambda_1)\lambda_1^2 \left(1 - \frac{\lambda_2}{\lambda_1}\right)\left(1 - \frac{X(\lambda_2)\lambda_2}{X(\lambda_1)\lambda_1}\right)$$

is positive.

For each conductivity model, we have, for $t \geqslant 0$,

$$C_{\mathrm{m}} \partial_t \|w(t)\|^2_{L^2(\Gamma)} + S_0 \|w(t)\|^2_{L^2(\Gamma)} \leqslant 0,$$

and

$$\|w(t)\|^2_{L^2(\Gamma)} \leqslant e^{-\frac{S_0}{C_{\mathrm{m}}}} \|w_0\|^2_{L^2(\Gamma)}. \tag{22}$$

Let $\Phi(u_0) := u(T)$. Writing the previous equation in $t = T$, we have

$$||\Phi(u_0) - \Phi(v_0)||_{L^2(\Gamma)} \leqslant e^{-\frac{S_0}{C_{\mathrm{m}}}T} ||u_0 - v_0||_{L^2(\Gamma)}, \tag{23}$$

with $e^{-\frac{S_0}{C_{\mathrm{m}}}T} < 1$. Therefore, Φ is a contraction on $L^2(\Gamma)$ and there exists a unique initial state u_0 satisfying Eq. (18). We have also proven the asymptotic convergence of any solution to problem (10) to the periodic solution. □

Remark 2. Note that the H^1 regularity is required on u and v so as their values are L^∞, thanks to the injection $H^s \hookrightarrow L^\infty$ for $s > \frac{d}{2}$. If we had considered the three dimensional case, then more regularity would have been necessary: u_0 and v_0 should be in $H^{3/2}(\Gamma)$ and G should be in $C_T(H^{3/2}(\Gamma))$.

Remark 3. If the operator $\mathcal{A}$ is coercive, with $\langle \mathcal{A}u, u\rangle > C_{\mathcal{A}} \|u\|^2_{L^2(\Gamma)}$ for all $u \in H^1(\Gamma)$, equation (20) becomes

$$C_{\mathrm{m}} \partial_t \|w\|^2_{L^2(\Gamma)} + S_0 \|w\|^2_{L^2(\Gamma)} + \langle S_{\mathrm{ep}}(t, u)u - S_{\mathrm{ep}}(t, v)v, u - v\rangle \leqslant -C_{\mathcal{A}} \|w\|^2_{L^2(\Gamma)}$$

and

$$\|w(t)\|^2_{L^2(\Gamma)} \leqslant e^{-\frac{S_0 + C_{\mathcal{A}}}{C_{\mathrm{m}}}} \|w_0\|^2_{L^2(\Gamma)}. \tag{24}$$

In this case, the convergence speed depends not only on the base conductivity of the membrane, but also on the shape of the cell and the extracellular conductivity, that are present in the definition of $\mathcal{A}$. We will detail in the next section a way to highlight the influence of these parameters for a circular cell.

4. Estimations of the convergence speed in the case of the circular cell.

4.1. Coercivity of the operator $\mathcal{A}$.

Under specific conditions on the cell shape, it is possible to refine the previous estimation of the convergence speed to periodic solutions defined in equation 24, by studying the operator $\mathcal{A}$. As many *in vitro* cells are nearly spherical, it is reasonable to consider a circular cell at first. We begin by proving the coercivity of $\mathcal{A}$ in concentric domains:

Proposition 1. *Let $\mathcal{O}_{\mathrm{c}}$ be a circular disk of radius R_1 and $\mathcal{O}_{\mathrm{e}}$ a concentric ring around $\mathcal{O}_{\mathrm{c}}$ of outer radius $R_2 > R_1$. Let $H^{1/2}_{\mathrm{p}}(\Gamma)$ be the space of functions of $H^{1/2}(\Gamma)$ with a zero mean value. Then the operator $(H^{1/2}_{\mathrm{p}}(\Gamma), \mathcal{A}) : u \mapsto \mathcal{A}u = \Lambda_{\mathrm{c}}(\mathrm{Id} + \Lambda_{\mathrm{e}}^{-1}\Lambda_{\mathrm{c}})^{-1}u$ with Λ_{e} and Λ_{c} defined by eqs. (12), is coercive.*

Proof. We proceed by explicitly defining the Dirichlet-to-Neumann operators. Let us recall the definition of Λ_e:

$$\Lambda_\mathrm{e} : u \mapsto -\sigma_\mathrm{e}\partial_{\boldsymbol{n}} v \quad \text{with} \quad \begin{cases} \Delta v = 0 \text{ in } \mathcal{O}_\mathrm{e}, \\ v = 0 \text{ on } \partial\Omega, \\ v = u \text{ on } \Gamma. \end{cases}$$

Expressing u and v with their Fourier transforms:

$$v = \sum_{k\in\mathbb{Z}^*} \alpha_k r^{|k|} e^{ik\theta} + \beta_k r^{-|k|} e^{ik\theta}, \; u = \sum_{k\in\mathbb{Z}^*} u_k e^{ik\theta},$$

with constant terms $u_0 = v_0 = 0$, the boundary conditions on Γ and $\partial\Omega$ lead to

$$\begin{cases} \alpha_k R_1^{|k|} + \beta_k R_1^{-|k|} = u_k, \\ \alpha_k R_2^{|k|} + \beta_k R_2^{-|k|} = 0, \end{cases} \Rightarrow \partial_{\boldsymbol{n}} v_k|_{R_1} = \frac{|k|}{R_1} \frac{R_2^{2|k|} + R_1^{2|k|}}{R_2^{2|k|} - R_1^{2|k|}} u_k.$$

Therefore

$$\Lambda_\mathrm{e}^{-1} : v_k e^{ik\theta} \mapsto \frac{R_1}{\sigma_\mathrm{e}\,|k|} \frac{R_2^{2|k|} - R_1^{2|k|}}{R_2^{2|k|} + R_1^{2|k|}} v_k e^{ik\theta}.$$

Using the same method for Λ_c leads to

$$\mathcal{A} = \Lambda_\mathrm{c}\left(\mathrm{Id} + \Lambda_\mathrm{e}^{-1}\Lambda_\mathrm{c}\right)^{-1} : u_k e^{ik\theta} \mapsto \frac{|k|}{R_1}\left(\frac{1}{\sigma_\mathrm{e}} \frac{R_2^{2|k|} - R_1^{2|k|}}{R_2^{2|k|} + R_1^{2|k|}} + \frac{1}{\sigma_\mathrm{c}}\right)^{-1} u_k e^{ik\theta}.$$

Then

$$\begin{aligned} \langle \mathcal{A}u, u\rangle &\geqslant \left(\frac{1}{\sigma_\mathrm{c}} + \frac{1}{\sigma_\mathrm{e}}\right)^{-1} \frac{1}{R_1} \sum_{k,l\in\mathbb{Z}} |k|\, u_k u_l \langle e^{ik\theta}, e^{il\theta}\rangle, \\ &= \left(\frac{1}{\sigma_\mathrm{c}} + \frac{1}{\sigma_\mathrm{e}}\right)^{-1} \frac{1}{R_1} \sum_{k,l\in\mathbb{Z}} |k|\, u_k u_l \int_0^{2\pi} e^{ik\theta} e^{-il\theta}\, \mathrm{d}\theta, \\ &= \left(\frac{1}{\sigma_\mathrm{c}} + \frac{1}{\sigma_\mathrm{e}}\right)^{-1} \frac{1}{R_1} \sum_{k\in\mathbb{Z}} |k|\, u_k^2, \\ &\geqslant \left(\frac{1}{\sigma_\mathrm{c}} + \frac{1}{\sigma_\mathrm{e}}\right)^{-1} \frac{1}{R_1} \|u\|^2_{H^{1/2}(\Gamma)}, \\ \langle \mathcal{A}u, u\rangle &\geqslant C_{\mathcal{A}} \|u\|^2_{L^2(\Gamma)} \end{aligned} \tag{25}$$

according to the definition of $\|\cdot\|_{H^{1/2}(\Gamma)}$ given by [18], p. 141, with

$$C_{\mathcal{A}} := \left(\frac{1}{\sigma_\mathrm{c}} + \frac{1}{\sigma_\mathrm{e}}\right)^{-1} \frac{1}{R_1}.$$

Therefore $\mathcal{A}$ is coercive. □

Remark 4. Remark that we cannot extend this property to functions with a non-zero mean value, as a consequence of the non-invertibility of Λ_c. For example, constant functions $u = u_0 \neq 0$ verify $\langle \mathcal{A}u, u\rangle = 0 < \|u\|^2_{H^{1/2}(\Gamma)}$.

Remark 5. Also note that it is possible to consider a cell embedded in a uniform electric field by making R_2 grow to infinity and considering only the case $|k| = 1$. Under these conditions, that are the most frequently found in experiments on cells,

the ratio $(R_2^{2|k|} - R_1^{2|k|})/(R_2^{2|k|} + R_1^{2|k|})$ tends to 1 and $\|u\|_{H^{1/2}(\Gamma)} = \|u\|_{L^2(\Gamma)}$, so that

$$\langle \mathcal{A}u, u\rangle = \left(\frac{1}{\sigma_c} + \frac{1}{\sigma_e}\right)^{-1} \frac{1}{R_1} \|u\|_{L^2(\Gamma)}.$$

Remark 6. It is possible to extend the coercive property of $\mathcal{A}$ to the three dimensional case, using spherical harmonic functions instead of usual Fourier series. Following the same computation, the estimation on the coercivity constant differs from the 2D case by a factor 2 :

$$\langle \mathcal{A}u, u\rangle \geqslant \left(\frac{1}{\sigma_c} + \frac{1}{\sigma_e}\right)^{-1} \frac{1}{2R_1} \|u\|^2_{H^{1/2}(\Gamma)}.$$

Remark 7. When the pulse g is constant, therefore periodic, this result shows the convergence of the X-model towards a static state (U^*, X^*) characterized by $X^* = \beta([U^*]_\Gamma)$ for both conductivity models.

Going back to problem (19), the coercivity of the operator $\mathcal{A}$ leads to

$$\frac{1}{2} C_m \partial_t ||w||^2_{L^2(\Gamma)} \leqslant -(S_0 + C_{\mathcal{A}})||w||^2_{L^2(\Gamma)}.$$

and for all $t \geqslant 0$

$$||w(t)||_{L^2(\Gamma)} < e^{-\frac{(S_0+C_{\mathcal{A}})}{C_m}t} ||w_0||_{L^2(\Gamma)}, \tag{26}$$

In this case, the convergence speed also depends on parameters included in the constant $C_{\mathcal{A}}$: the extracellular conductivity and the size of the cell. These dependencies will be illustrated in the next section.

4.2. **Numerical validation.** In order to solve numerically equation (2), the same scheme as in [6] was used. It is based on a method developped by Cisternino and Weynans [2], using second order finite differences for spatial discretization and adding unknowns at the intersection points of the interface Γ on the cartesian grid for a special treatment of fluxes. The details of the method are explained and its convergence proven in a another previous publication dedicated to the numerical aspects of the problem [8].

Simulations were all performed in a two dimensional domain with the parameters presented in table 1. Biological parameters of the simulations are taken from the articles of Neu *et al.* [3]. The chosen cell size is however smaller in order to match the experiments. Dynamics of electroporation (τ_{ep}) and the maximal value of conductivity (S_1) were set during a previous fit of our model with the results of Neu *et al.*

Since the numerical method is based on a cartesian grid, the simulated domain is a square $[x_{min}, x_{max}] \times [y_{min}, y_{max}]$ that is large enough compared to the radius of the cell, which is circular.

The chosen boundary conditions simulate a uniform electric field of amplitude E. It consists in a Dirichlet condition in the x direction, and a homogeneous Neumann condition in the y direction. In this case, effects due to the presence of the square-shaped boundary on the transmembrane potential difference (ΔTMP) can be neglected.

The problem to solve reads

$$\begin{cases} \Delta U = 0 & \text{in } \mathcal{O}_{\mathrm{e}} \cup \mathcal{O}_{\mathrm{c}}, \\ U(t=0,x,y) = 0 & \text{in } \Omega, \\ [\sigma \partial_{\boldsymbol{n}} U] = 0 & \text{on } \Gamma, \\ C_{\mathrm{m}} \partial_t [U] + S_{\mathrm{m}}(t,[U])\,[U] = \sigma_{\mathrm{c}} \partial_{\boldsymbol{n}} U|_{\Gamma^-} & \text{on } \Gamma \\ U(t,x,y) = Ex & \text{if } x = x_{\min} \text{ or } x = x_{\max},\ \forall t > 0, \\ \partial_{\boldsymbol{n}} U(t,x,y) = 0 & \text{if } y = y_{\min} \text{ or } y = y_{\max},\ \forall t > 0. \end{cases} \tag{27}$$

TABLE 1. Parameters of numerical simulations, that are mostly taken from [6]. EP stands for electropermeabilization, EPd for electropermeabilized.

Variable	Symbol	Value	Unit
Biological parameters:			
Intracellular conductivity	σ_{c}	0.455	S/m
Capacitance	C_{m}	1	F/m^2
Membrane surface conductivity	S_0	1.9	S/m^2
Cell radius	R_1	6	μm
Specific parameters of the models:			
EP threshold	V_{th}	0.2	V
EP switch speed	k_{ep}	40	V^{-1}
EP characteristic time	τ_{ep}	1×10^{-6}	s
EPd membrane surface conductivity	S_1	1×10^{6}	S/m^2
Numerical parameters:			
Simulation box size	L	30	μm
Grid points (each side)	N	100	
Time step	Δt	200	ns
Pulse parameters:			
Pulse duration	T_{p}	10	μs
Pulse period	T	20	μs
Intensity	E	40	kV/m
Duration of simulation	T_{f}	1000	μs

4.2.1. *Linear model.* Before studying the influence of the electropermeabilization model on the convergence towards a periodic solution, we will focus on the variation of the coercivity constant $C_{\mathcal{A}}$ with the extracellular conductivity σ_{e}. In this section, we will consider a constant surface conductivity of the membrane.

The chosen pulse parameters to study the linear effects are not commonly used. Using a clinical pulse protocol with a linear model does not lead to relevant convergence results since pulses are separated by a time that is long enough to let

the cell retrieve its initial state. The solution is therefore already periodic for any pulse intensity. To prevent this, the pulses frequency was considerably augmented to avoid the complete discharge of the membrane between two pulses. Moreover, the membrane capacitance C_{m} was also changed to 1 (instead of $\sim$0.01) to extend the duration of the charge and discharge of the membrane. This allows also direct comparison with the estimation of $C_{\mathcal{A}}$ in equation (25).

The periodic solution $\overline{u}$ to problem (18) is obtained by performing long-time simulations of 50 periods, and verifying that the last obtained period does not vary from the previous one more than a ratio of 10^{-10} : if T_{f} designates the final time of the simulation,

$$\frac{\displaystyle\int_{T_{\mathrm{f}}-T}^{T_{\mathrm{f}}} \|u(t)-u(t-T)\|_{H^{1/2}(\Gamma)}\ \mathrm{d}t}{\displaystyle\int_{T_{\mathrm{f}}-T}^{T_{\mathrm{f}}} \|u(t)\|_{H^{1/2}(\Gamma)}\ \mathrm{d}t} < 10^{-10}. \tag{28}$$

Under these conditions, the last period is considered as the periodic solution. We then compute the L^2 error

$$e(t) := \|\overline{u}(t)-u(t)\|_{L^2(\Gamma)}.$$

The error is fitted with an exponential function

$$e(t) \sim A\exp^{-Bt}, \tag{29}$$

where A and B are constants, as illustrated in figure 2. The constant B can be considered as an estimation of the convergence speed $C_{\mathcal{A}}$.

The process is repeated for different extracellular conductivities σ_{e} and radiuses R_1. The Fourier coefficients of the solution are computed to check whether the influence of the square-shaped simulation box is important or not. All simulations showed that the greatest Fourier coefficient $u_k, |k| \neq 1$ of the solution is $u_{|3|}$, 1000 times lower than the main harmonic $u_{|1|}$. Figure 3 shows that the dependency on σ_{e} and R_1 of the decay rate $B \leqslant S_0 + C_{\mathcal{A}}$ is satisfied. The evaluated constant B has the same order of magnitude as the estimation of $C_{\mathcal{A}}$ in (25).

4.2.2. *Static conductivity model.* The same method was used to study the decay rate to periodic solutions when the membrane conductivity is a non-linear function of the transmembrane potential difference. Simulations showed that the decay of the difference between the solution and the periodic state is still an exponential function of time:

$$e(t) \sim e^{-Ct}e(0).$$

even in the non-linear case. The constant C still includes the base conductivity of the membrane and the coercivity of the operator $\mathcal{A}$. We propose to note $C = S_0 + C_{\mathcal{A}} + C_{S_{\mathrm{ep}}}$, where $C_{S_{\mathrm{ep}}}$ accounts for the non-linearity of the conductivity.

Figure 4 shows the behaviour of the quantity C when the extracellular conductivity varies, for the static model of membrane conductivity. The dependency on σ_{e} is similar to the linear case, the difference being only a constant factor. This can be explained by the increase in the maximum value of the ΔTMP that is obtained for each simulation. Lower conductivities induce a limited rise of the ΔTMP, contrary to high conductivities, for which the ΔTMP is close to the threshold voltage. Then the Lipschitz constant of $\lambda \mapsto \lambda S_{\mathrm{ep}}$ vary accordingly to the maximum value of the

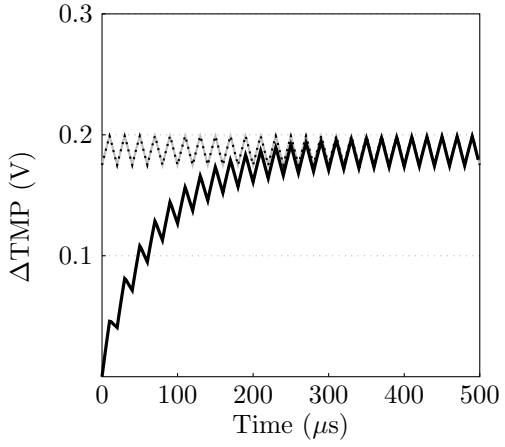

(a)

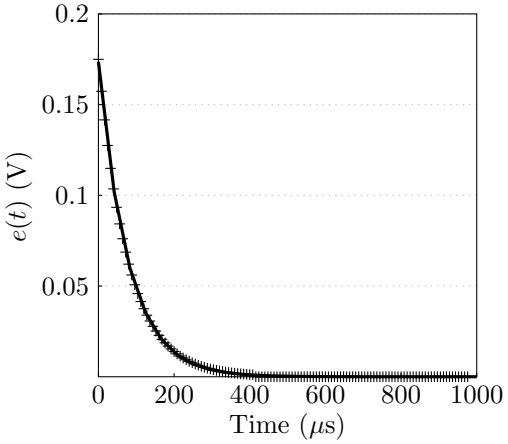

(b)

FIGURE 2. 2(a) : Transmembrane potential difference (solid) and periodic solution (dotted) of the linear problem, with $\sigma_e = 0.2$ S.m^{-1}. 2(b) : Fit of the L^2 error $e(t)$ between the ΔTMP and the periodic solution, giving the constant $C_{\mathcal{A}}$.

ΔTMP λ_m:

$$C_{S_{ep}} \leqslant S_1 \max_{\lambda} |(\lambda\beta(\lambda))'| = S_1 \left(\beta(\lambda_m) + |\lambda_m| \beta'(\lambda_m)\right), \tag{30}$$

since $\lambda_m < V_{th}$ in all our simulations. Figure 5 shows that the simulation results are in agreement with this estimation, although the proposed constant for the β model is one order of magnitude higher.

4.2.3. *Dynamical model.* Figure 6 shows a different evolution of the non-linearity for the dynamical model. For lower conductivities, the behaviour is the same as the static case, since the applied pulse train is not sufficient to reach the voltage

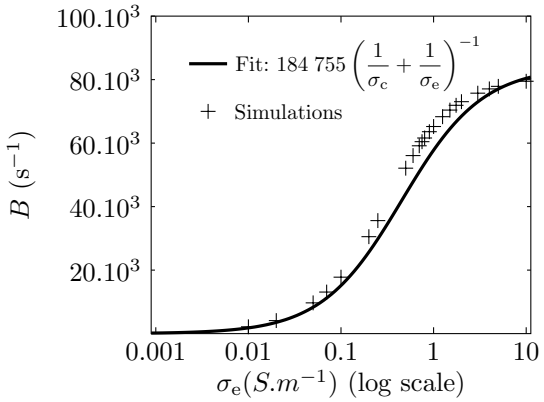

(a)

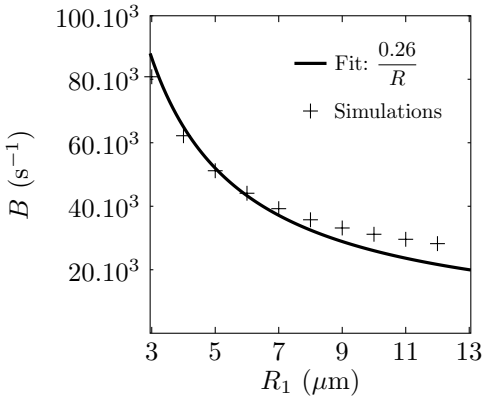

(b)

FIGURE 3. Linear conductivity model : evaluated decay rate B of the L^2 error depending on the extracellular conductivity σ_e with $R_1 = 6$ μm (3(a)) and depending on the radius of the cell R_1 with $\sigma_e = 0.5$ S/m (3(b)). The first fitting constant has the same order of magnitude as $R_1^{-1} \sim 167\,000$. The other constant is of the order of $(\sigma_e^{-1} + \sigma_c^{-1})^{-1} \sim 0.24$.

threshold. However, as the extracellular conductivity rises, a drop of the convergence speed occurs, which depends on the dynamics of X. If τ_{ep} is low enough, the dynamical model has a behaviour which is the same as the β-model, whereas slower dynamics do not affect the convergence speed more than the linear constant.

Since the choice of the model has a quantitative impact on the convergence speed to a periodic state, it may be important to translate the results of figure 6 in terms of pulse application. Figure 7 gives the number of pulses that are necessary to obtain a periodic response of the cell. This number is computed so as the solution is no more than 1% different from the periodic solution in $L^2(\Gamma)$ norm:

$$N(\sigma_e) := \left\lceil \frac{2 \ln 10}{C(\sigma_e) T} \right\rceil \tag{31}$$

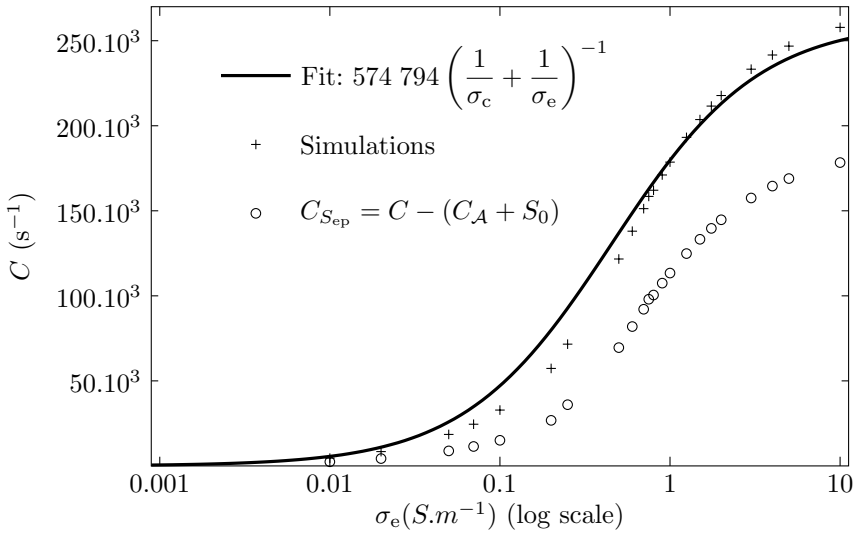

FIGURE 4. Evaluated convergence rate to the periodic solution for the β-model $S_{\mathrm{m}}(\lambda) = S_0 + S_1\beta(\lambda)$. The contribution of the non-linearity $C_{S_{\mathrm{ep}}}$ has also been plotted, using values of $C_{\mathcal{A}}$ from figure 3.

It is shown that for the permeabilizing cases ($\sigma_{\mathrm{e}} \geqslant 0.3$ S/m), three to four additional pulses are required for the dynamical model to achieve convergence, compared to the static model for which two pulses are sufficient. If it is intended to obtain a conductivity which corresponds to the periodic state, then considering only a static model of conductivity can lead to a lower level of permeabilization than expected.

We emphasize that these modeling results were obtained on a circular cell with uncommon parameters. However, when computing the electric potential with experimental pulse parameters (400 V/cm, 100 μs), we obtain convergence towards a periodic state in no more than two or three pulses, which is below the usual eight pulses used to permeabilize cell [4, 15, 17]. As the models are not fully calibrated yet, these results are only qualitative, and the difference between the static and dynamic models may be different for other electric pulses.

5. **Conclusion.** In this paper we study the evolution of solutions to several models of electropermeabilization derived from Kavian et al. [6] in the specific case of periodic sources. We show existence and uniqueness of periodic solutions, as well as convergence to these solutions given any initial condition. Using a simulation tool that was created specifically to solve electropermeabilization problems, we validate theoretical estimations of the convergence speed to periodic solutions. In particular, we show that the shape of the cell has a strong influence on this speed.

We emphasize that static models of membrane conductivity give an overestimation of the convergence speed, compared to the dynamical model. Since the permeabilization is linked to the conductivity, those models predict a higher permeabilization level of the cell for short pulse treatments. The number of pulses needed to obtain a given conductivity is then lower than predictions of the dynamical model, and the cell could not be actually porated.

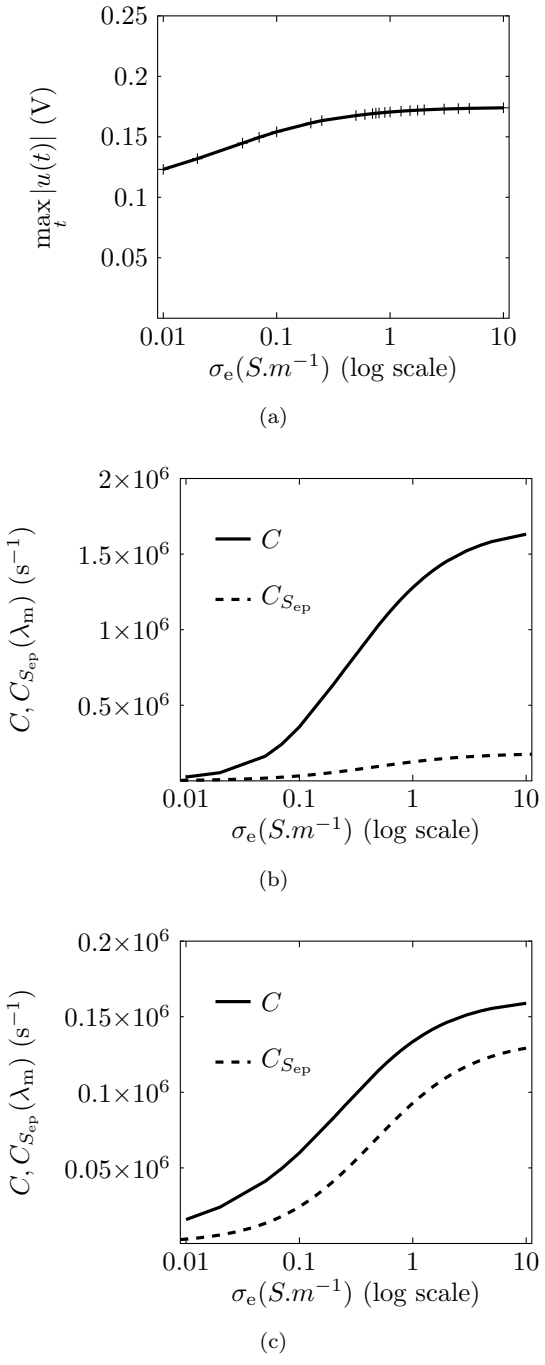

FIGURE 5. 5(a): Maximum ΔTMP during simulations for the β static model. 5(b): Comparison of simulated and estimated Lipschitz constant $C_{S_{ep}}$ as defined in 30. Solid line : difference between non-linear and linear decay rates. Dashed line : estimations from eq (30) with λ_m from figure 5(a).

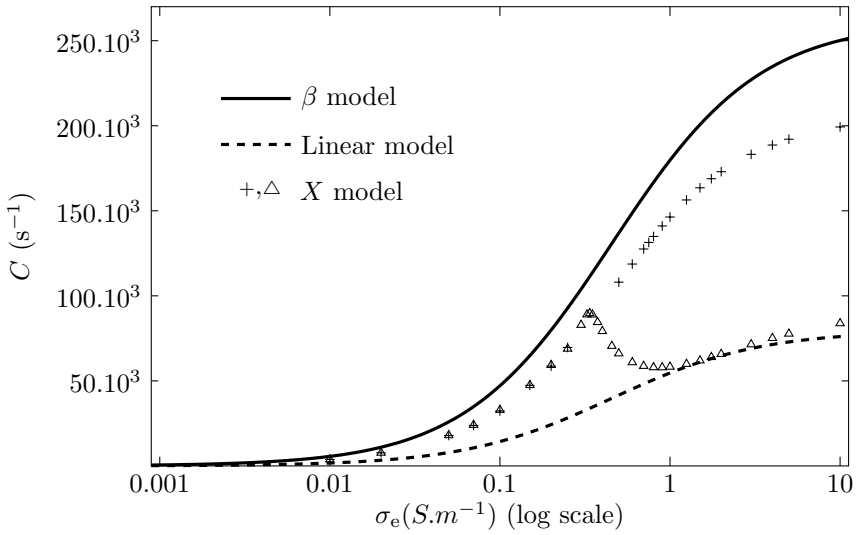

FIGURE 6. Decay rate to the periodic solution for the dynamical case $S_{\mathrm{m}}(\lambda) = S_0 + S_1 X(t)$, compared to the evaluations already performed for the linear and the β models. Simulations of the dynamical model were made for several characteristic durations: $\tau_{\mathrm{ep}} = 1\ \mu s(+),\ \tau_{\mathrm{ep}} = 10\ \mu s(\triangle)$.

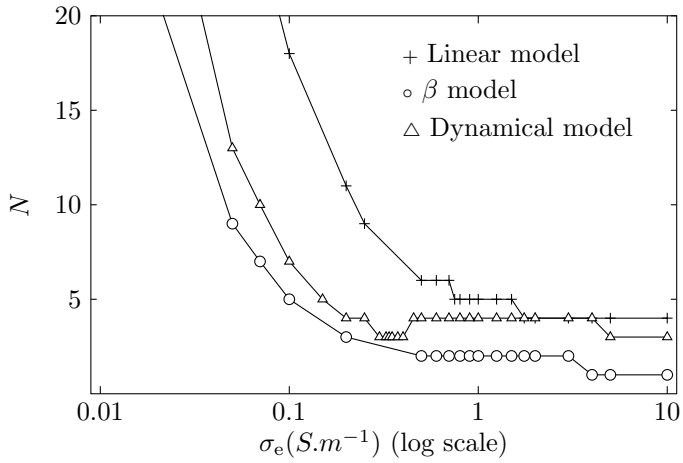

FIGURE 7. Number of pulses $N(\sigma_{\mathrm{e}})$ given by eq. (31) for the linear, β and dynamical models.

Acknowledgments. This study has been carried out in the frame of Investments for the future Programme IdEx Bordeaux CPU (ANR-10-IDEX-03-02). The authors have been partly granted by the French national agency throughout the research projects INTCELL (2010-BLAN-916-04) and MEMOVE (2011-BS01-006-01). Numerical experiments presented in this paper were carried out using the

PLAFRIM experimental testbed, being developed under the Inria PlaFRIM development action with support from LaBRI and IMB and other entities: Conseil Régional d'Aquitaine, FeDER, Université de Bordeaux and CNRS (see https://plafrim.bordeaux.inria.fr/). This work was partly performed in the scope of the European Associated Laboratory EBAM.

REFERENCES

[1] L. Calmels, B. Al-Sakere, J. P. Ruaud, A. Leroy-Willig and L. M. Mir, In vivo MRI follow-up of murine tumors treated by electrochemotherapy and other electroporation-based treatments, *Technology in Cancer Research and Treatment*, **11** (2012), 561–570.

[2] M. Cisternino and L. Weynans, A parallel second order cartesian method for elliptic interface problems, *Communications in Computational Physics*, **12** (2012), 1562–1587.

[3] K. DeBruin and W. Krassowska, Modelling electroporation in a single cell. I. Effects of field strength and rest potential, *Biophysical Journal*, **77** (1999), 1213–1224.

[4] A. Gothelf, L. M. Mir and J. Gehl, Electrochemotherapy: Results of cancer treatment using enhanced delivery of bleomycin by electroporation, *Cancer Treatment Reviews*, **29** (2003), 371–387.

[5] R. P. Joshi, Q. Hu and K. H. Schoenbach, Dynamical modeling of cellular response to short-duration, high-intensity electric fields, *Dielectrics and Electrical Insulation, IEEE Transactions on*, **10** (2003), 778–787.

[6] O. Kavian, M. Leguèbe, C. Poignard and L. Weynans, "Classical" electropermeabilization modeling at the cell scale, *Journal of Mathematical Biology*, **68** (2014), 235–265.

[7] M. Leguèbe, *Modélisation de L'électroperméabilisation à L'échelle Cellulaire (French)*, PhD thesis, Université de Bordeaux, 2014.

[8] M. Leguèbe, C. Poignard and L. Weynans, *A Second-Order Cartesian Method for the Simulation of Electropermeabilization Cell Models*, Technical Report RR-8302, Inria, 2013.

[9] M. Leguèbe, A. Silve, L. M. Mir and C. Poignard, Conducting and permeable states of cell membrane submitted to high voltage pulses: Mathematical and numerical studies validated by the experiments, *Journal of Theoretical Biology*, **360** (2014), 83–94.

[10] J. Li and H. Lin, The current-voltage relation for electropores with conductivity gradients, *Biomicrofluidics*, **4** (2010), 13206.

[11] L. M. Mir, Electrogenetransfer in clinical applications, *Wiley-VCH Verlag GmbH & Co. KGaA,* (2006), 219–226.

[12] O. M. Nesin, O. N. Pakhomova, S. Xiao and A. G. Pakhomov, Manipulation of cell volume and membrane pore comparison following single cell permeabilization with 60- and 600-ns electric pulses, *Biochimica et Biophysica Acta - Biomembranes*, **1808** (2011), 792–801.

[13] J. Neu and W. Krassowska, Asymptotic model of electroporation, *Physical Review E*, **53** (1999), 3471–3482.

[14] V. Péron, *Modélisation Mathématique de Phénomènes Électromagnétiques dans des Matériaux à Fort Contraste (French)*, PhD thesis, Université Rennes 1, 2009.

[15] B. Poddevin, S. Orlowski, J. Belehradek and L. M. Mir, Very high cytotoxicity of bleomycin introduced into the cytosol of cells in culture, *Biochemical Pharmacology*, **42** (1991), S67–S75.

[16] C. Poignard, Approximate transmission conditions through a weakly oscillating thin layer, *Mathematical Methods in the Applied Sciences*, **32** (2009), 435–453.

[17] G. Pucihar, J. Krmelj, M. Reberšek, T. B. Napotnik and D. Miklavčič, Equivalent pulse parameters for electroporation, *IEEE Trans Biomed Eng*, **58** (2011), 3279–3288.

[18] J. Saranen and G. Vainikko, *Periodic Integral and Pseudodifferential Equations with Numerical Approximation*, Springer Monographs in Mathematics, Springer-Verlag, Berlin, 2002.

[19] S. Šatkauskas, F. M. André, M. F. Bureau, D. Scherman, D. Miklavčič and L. M. Mir, Electrophoretic component of electric pulses determines the efficacy of in vivo DNA electrotransfer, *Human Gene Therapy*, **16** (2005), 1194–1201.

[20] A. Silve, A. Ivorra and L. M. Mir, Detection of permeabilisation obtained by micropulses and nanopulses by means of bioimpedance of biological tissues, in *Proceedings of the 5th European Conference on Antennas and Propagation (EUCAP)*, (2011), 3164–3167.

Received November 05, 2013; Accepted January 05, 2015.

E-mail address: leguebe@mps.mpg.de